Available online at www.sciencedirect.com

SciVerse ScienceDirect

journal homepage: www.elsevier.com/locate/jmbbm

Research paper

Nanoindentation of osteonal bone lamellae

Anna Faingold[a], *Sidney R. Cohen*[b], *H. Daniel Wagner*[a,*]

[a] *Department of Materials and Interfaces, Weizmann Institute of Science, Rehovot 76100, Israel*
[b] *Chemical Research Support, Weizmann Institute of Science, Rehovot 76100, Israel*

ARTICLE INFO

Article history:
Received 17 August 2011
Received in revised form
4 January 2012
Accepted 14 January 2012
Published online 31 January 2012

Keywords:
Lamellar bone
Anisotropy
Nanoindentation
Mechanical properties
Structure
Osteon

ABSTRACT

Variations in Young's modulus of individual lamellae around a single bone osteon have been measured in three orthogonal planes by nanoindentation. The objective of these measurements was to establish a correlation between the mechanical properties and the microstructure of the osteonal lamellae. When indentation was performed in a plane perpendicular to the osteon axis (OA), the modulus of the lamella closest to the canal appears to be higher than the modulus of all other lamellae. No such difference was observed in planes parallel to the OA. However, in the parallel planes, an unexpected asymmetry in modulus was detected on opposing sides of the canal, potentially supporting the validity of the rotated plywood structure model of bone lamellae. Finally, based on the experimentally measured Young's modulus values, most osteonal lamellae appear to exhibit structural anisotropy.

1. Introduction

The structure and mechanical properties of bone lamellae at the nano-level have been widely studied in recent years; however their full understanding remains elusive. Optical microscopy studies revealed different thicknesses as well as evidence for structural variations of the lamella in the secondary osteon structure (Ascenzi and Lomovtsev, 2006; Turner et al., 1995; Weiner et al., 1997). These differences can be related to the organization of the mineralized collagen fibrils, which are the basic components of these lamellae. A model for the basic organizational structure of osteonal bone consists of ordered layers of mineralized fibrils, with different thicknesses, which undergo a progressive rotation with respect to neighboring layers (Giraud-Guille, 1988; Wagermaier et al., 2006; Weiner and Traub, 1986). This "rotated plywood structure" has gradually gained credibility, as it is supported by structural studies performed in a synchrotron micro-beam (Wagermaier et al., 2006). An alternative model raises the possibility that the lamellation is due to the alternation of collagen-rich and collagen-poor units, all having an interwoven texture of fibrils (Marotti, 1993).

Theoretical and experimental efforts to understand the structure and symmetry of the elementary units of lamellar bone are therefore still being pursued. Theoretical calculations have led to estimations of the mechanical properties of parallel bone (Akiva et al., 1997; Seto et al., 2008) (where mineralized fibrils are all oriented in the same direction), single lamellae (Franzoso and Zysset, 2009; Reisinger et al., 2010; Yoon and Cowin, 2008) and lamellar bone (Akiva et al., 1998) in the three orthogonal directions. Various studies of the structure (Ascenzi and Lomovtsev, 2006; Kazanci et al., 2007; Wagermaier et al., 2006; Weiner et al., 1997), as well as mechanical properties using both

* *Corresponding author.* Tel.: +972 89342594.
E-mail address: daniel.wagner@weizmann.ac.il (H.D. Wagner).

1751-6161/$ - see front matter
doi:10.1016/j.jmbbm.2012.01.014

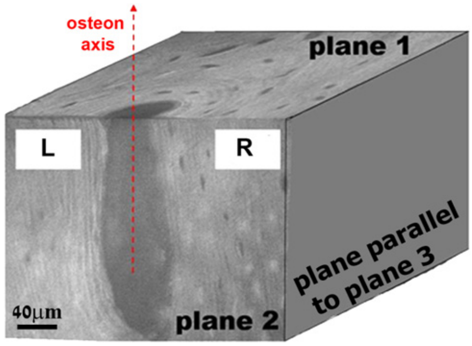

Fig. 1 – 3D view of optical microscopy images of an osteon after exposure of two perpendicular planes (plane 1 and plane 2). L and R represent the left and the right side of the osteon, respectively, as they appear in the text.

nanoindentation (Fan et al., 2002; Franzoso and Zysset, 2009; Gupta et al., 2006; Hoffmann et al., 2006; Rho et al., 1999) and ultrasonic techniques (Raum et al., 2006; Turner et al., 1995) can be found in the literature, but most of them are confined to one plane of the bone structure. Reports that include information on more than one plane generally use separate samples for each plane (Fan et al., 2002; Hoffmann et al., 2006). The few studies that investigated two or more planes of a single osteon found anisotropy in the mechanical properties (Franzoso and Zysset, 2009; Reisinger et al., 2011; Turner et al., 1995; Wang et al., 2007). An additional work studied structural differences using Raman spectroscopy (Kazanci et al., 2007). Even fewer studies exist at a resolution of a single lamella (Gupta et al., 2006; Kazanci et al., 2007; Reisinger et al., 2011). The exact 3D structure and mechanical properties of these elementary units are therefore still unknown. The present study investigates this issue by isolating, successively exposing, and measuring the mechanical properties in orthogonal planes of a single osteon at a resolution of a single lamella, using a cubic specimen (Fig. 1).

2. Materials and methods

2.1. *Specimen preparation*

To study the mechanical properties of osteonal bone, a sample from the fresh frozen subchondral part (upper part) of the metacarpal bone of a 5 year old male horse was selected. Equine and human osteons are of comparable sizes, namely about 200 μm in diameter. The sample was cut using a Minitom cutting instrument (Struers). A cubic sample of about 0.5 cm in side was then ground and polished manually on a plane perpendicular to the bone axis ('plane 1', see Fig. 1) with SiC papers of grit 360, 800 and 4000, then with diamond powder of 1 μm and 0.25 μm and finally with 0.05 μm alumina suspension. After rinsing, the samples were kept dry (in ambient conditions) for at least 24 h before measurement.

After a complete study of plane 1, a second plane ('plane 2') and a third plane ('plane 3'), both parallel to the bone axis, were successively exposed by grinding and polishing the same osteon, following a procedure identical to that for plane 1. This is summarized in Fig. 2. Plane 3 was exposed only after the study of plane 2 was completed.

The angle between each pair of planes was 90°, with a maximum deviation of 2.5%.

Plane 1 was defined as perpendicular to the osteon axis (OA) since osteonal canals were circular in this plane even though, osteons are never perfectly aligned in the bone tissue.

2.2. *Nanoindentation*

Nanoindentation measurements were performed with an XP-Nanoindenter (Agilent) employing the DCM measuring head, and using the Nanovision^{TM} feature, allowing placement of indentations based on high resolution topographical scans over the specified area using the indenter tip. Scanning was performed in a profilometric mode, by measuring the displacement of the tip at a constant force of 1.3–1.5 μN, a procedure which results in a topographical image of the surface. Young's modulus (E) and hardness (H) were calculated using the Oliver and Pharr method (Oliver and Pharr, 1992). Note that as defined by Oliver and Pharr, the nanoindentation hardness H may differ from that found in microindentation, as here it is the maximum load applied divided by projected contact area at that load whereas in microindentation it is the maximum load divided by area determined from residual impression. All measurements were performed in continuous stiffness measurement (CSM) mode, which provides continuous measurements of the mechanical properties during loading and not just at the point of initial unloading (maximum displacement). This is accomplished by superimposing a small (1–2 nm) oscillation on the quasistatic loading curve, while lock-in detection of the response allows calculation of values for Young's modulus and hardness continuously during loading, still in accordance with the Oliver and Pharr method. This permits setting ultimate indentation depth to the minimal value where surface effects no longer dominate the response, optimizing spatial resolution while ensuring reliability of the result. All indentations as well as surface scanning were performed with a Berkovich diamond indenter.

The indentations were made as follows: (i) loading the sample at a rate of 10 nm/s, with 2 nm harmonic modulations at frequency of 75 Hz until the applied force reached 500 μN (resulting in residual indents of about 1 μm in width); (ii) 5 s holding period (iii) unloading at a rate of 100 μN/s.

A combined effect of thermal drift and creep at a rate of about 1.3 nm/s was revealed at step (ii). However, it has been shown that CSM values are insignificantly affected by creep and thermal drift, as very short time periods are involved (Rar et al., 2005). In the present case, a creep of less than 0.0173 nm is expected for each 2 nm cycle (1.3 nm/s creep rate divided by 75 Hz cycle period length), resulting in an error of about 0.03% in Young's modulus for an overall indentation depth below 60 nm and even less as the depth increases. The tip area function calibration was performed using fused silica as a standard to ascertain calibration of the machine and diamond tip. This calibration resulted in average Young's modulus of 71.7 ± 0.3 GPa for fused silica, in agreement with the standard value of 72 GPa.